

Radiatively Induced Neutrino Mass Model with Flavor Dependent Gauge Symmetry

SangJong Lee,¹ Takaaki Nomura,^{1,*} and Hiroshi Okada^{2,†}

¹*School of Physics, KIAS, Seoul 02455, Korea*

²*Physics Division, National Center for Theoretical Sciences, Hsinchu, Taiwan 300*

(Dated: March 11, 2022)

Abstract

We study a radiative seesaw model at one-loop level with a flavor dependent gauge symmetry $U(1)_{\mu-\tau}$, in which we consider bosonic dark matter. We also analyze the constraints from lepton flavor violations, muon $g-2$, relic density of dark matter, and collider physics, and carry out numerical analysis to search for allowed parameter region which satisfy all the constraints and to investigate some predictions. Furthermore we find that a simple but adhoc hypothesis induces specific two zero texture with inverse mass matrix, which provides us several predictions such as a specific pattern of Dirac CP phase.

Keywords:

*Electronic address: nomura@kias.re.kr

†Electronic address: macokada3hiroshi@cts.nthu.edu.tw

I. INTRODUCTION

The observation of neutrino oscillation confirms at least two non-zero masses of active neutrinos indicating physics beyond the standard model (SM) to generate the neutrino masses. Radiative seesaw models are one of the attractive candidate to generate the neutrino masses where a neutrino mass matrix is induced at loop level and a dark matter (DM) candidate can be included as a particle propagating inside a loop diagram for generating neutrino mass. It is also interesting to include flavor dependent gauge symmetry with which we can obtain predictive structure of neutrino mass matrix [1, 2].

One of the interesting flavor dependent $U(1)$ gauge symmetry is the $U(1)_{\mu-\tau}$ which can induce sizable deviation of muon anomalous magnetic dipole moment from SM prediction, Δa_μ , where experimental observation indicates $\Delta a_\mu \simeq O(10^{-9})$ suggesting discrepancy from the SM value [3]. In addition, some interesting phenomenologies regarding the $U(1)_{\mu-\tau}$ are investigated, e.g. in Refs. [4–18]. The $U(1)_{\mu-\tau}$ symmetry also can constrain the structure of Majorana mass matrix of neutrinos giving predictability for neutrino sector. However, it is not so trivial when the active neutrino mass matrix is generated via radiative seesaw mechanism. We then apply the $U(1)_{\mu-\tau}$ gauge symmetry in a radiative seesaw model and investigate prediction in neutrino mass matrix.

In this paper, we construct a radiative seesaw model with $U(1)_{\mu-\tau}$ gauge symmetry and Z_2 symmetry in which we introduce exotic $SU(2)_L$ doublet leptons with $U(1)_{\mu-\tau}$, a Z_2 even singlet scalar field, and Z_2 odd triplet and singlet scalar fields. In the model, active neutrino mass matrix is generated at one loop level where Z_2 odd particles propagate inside a loop diagram. Furthermore we have DM candidate which is the lightest Z_2 odd neutral particle. Then global numerical analysis is carried out to search for allowed parameter region and to investigate some predictions in the model, taking into account constraints from charged lepton flavor violation (cLFV), Δa_μ , and relic density of DM. In addition, we find that structure of the Dirac mass matrix of exotic lepton determines that of the active neutrino mass matrix when we apply assumptions *i*) degenerate masses for exotic leptons, or *ii*) some vanishing Yukawa couplings which are associated with interactions among SM leptons, exotic leptons and exotic scalars. In that case, we have two zero texture of the neutrino mass matrix which provides some predictions in neutrino oscillation experiments.

This paper is organized as follows. In Sec. II, we introduce our model and discuss some

	Leptons								
Fermions	L_{Le}	$L_{L\mu}$	$L_{L\tau}$	e_R	μ_R	τ_R	L'_e	L'_μ	L'_τ
$SU(3)_C$	1	1	1	1	1	1	1	1	1
$SU(2)_L$	2	2	2	1	1	1	2	2	2
$U(1)_Y$	$-\frac{1}{2}$	$-\frac{1}{2}$	$-\frac{1}{2}$	-1	-1	-1	$-\frac{1}{2}$	$-\frac{1}{2}$	$-\frac{1}{2}$
$U(1)_{\mu-\tau}$	0	1	-1	0	1	-1	0	1	-1
Z_2	+	+	+	+	+	+	-	-	-

TABLE I: Field contents of fermions and their charge assignments under $SU(2)_L \times U(1)_Y \times U(1)_{\mu-\tau} \times Z_2$.

	VEV $\neq 0$		Inert	
Bosons	Φ	φ	Δ	S
$SU(2)_L$	2	1	3	1
$U(1)_Y$	$\frac{1}{2}$	0	1	0
$U(1)_{\mu-\tau}$	0	1	0	0
Z_2	+	+	-	-

TABLE II: Field contents of bosons and their charge assignments under $SU(2)_L \times U(1)_Y \times U(1)' \times Z_2$, where $SU(3)_C$ singlet for all bosons.

phenomenologies such as neutrino mass matrix, lepton flavor violation, and some processes induced by Z' interactions. The numerical analysis is carried out in Sec. III to search for parameter region satisfying experimental constraints and to obtain some prediction for neutrino mass matrix. Finally we summarize the results in Sec. IV.

II. MODEL, PARTICLE PROPERTIES AND PHENOMENOLOGY

In this section, we introduce our model and discuss some phenomenologies. As extra symmetries, local $U(1)_{\mu-\tau}$ and discrete Z_2 symmetries are added. In the fermion sector, we introduce $SU(2)_L$ doublet vector like fermions $L'_{e,\mu,\tau} \equiv [N, E]_{e,\mu,\tau}^T$, and impose a flavor dependent gauge symmetry $U(1)_{\mu-\tau}$ as summarized in Table I. Also Z_2 odd parity is imposed

for this new fermion in order to discriminate the SM model leptons with $SU(2)_L$ and forbid the mixing between them.¹ In the scalar sector, we add an $SU(2)_L$ triplet inert scalar Δ , real singlet inert scalar S , and singlet scalar φ to the SM Higgs Φ as summarized in Table II. Notice here the Higgs doublet Φ (that spontaneously breaks electroweak symmetry), the $SU(2)$ singlet field φ (that spontaneously break $U(1)_{\mu-\tau}$ symmetry), have the vacuum expectation values (VEVs), which are respectively symbolized by $v/\sqrt{2}$, $v'/\sqrt{2}$, and Z_2 odd parity is also imposed for the inert scalars Δ and S to forbid the tree level neutrino masses through VEVs. Therefore the lightest neutral scalar boson with Z_2 odd parity can be a DM candidate.

Yukawa interactions and scalar potential: Under these fields and symmetries, the renormalizable Lagrangians for quark and lepton sector are given by

$$\begin{aligned}
-\mathcal{L}_L = \sum_{\ell=e,\mu,\tau} & [y_\ell \bar{L}_{L_\ell} \Phi \ell_R + y_{S_\ell} \bar{L}_{L_\ell} L'_{R_\ell} S + M_\ell \bar{L}'_{L_\ell} L'_{R_\ell}] \\
& + y_{\Delta_1} \bar{L}_{L_e}^C (i\sigma_2) \Delta L'_{L_e} + y_{\Delta_2} \bar{L}_{L_\tau}^C (i\sigma_2) \Delta L'_{L_\mu} + y_{\Delta_3} \bar{L}_{L_\mu}^C (i\sigma_2) \Delta L'_{L_\tau} \\
& + y_{E_1} \varphi^* \bar{L}'_{L_e} L'_{R_\mu} + y_{E_2} \varphi \bar{L}'_{L_e} L'_{R_\tau} + \text{c.c.},
\end{aligned} \tag{II.1}$$

where σ_2 is the second Pauli matrix, and again $L' \equiv [N, E]^T$.

We parametrize the scalar fields as

$$\Phi = \begin{bmatrix} w^+ \\ \frac{v+\phi+iz}{\sqrt{2}} \end{bmatrix}, \quad \eta = \begin{bmatrix} \eta^+ \\ \frac{\eta_R+i\eta_I}{\sqrt{2}} \end{bmatrix}, \quad \Delta = \begin{bmatrix} \frac{\Delta^+}{\sqrt{2}} & \Delta^{++} \\ \Delta^0 & -\frac{\Delta^+}{\sqrt{2}} \end{bmatrix}, \quad \Delta_0 = \frac{\Delta_R + i\Delta_I}{\sqrt{2}}, \quad \varphi = \frac{v' + \rho + iz'}{\sqrt{2}}, \tag{II.2}$$

where $v \simeq 246$ GeV is VEV of the Higgs doublet, and w^\pm , z , and z' are respectively Nambu-Goldstone boson(NGB) which are absorbed by the longitudinal component of W , Z , and Z' boson; Z' boson comes from $U(1)_{\mu-\tau}$ gauge field. Then we have two neutral boson mass matrices $m_{\rho\phi}^2$ and $m_{S\Delta}^2$ in the basis of $[\rho, \phi]^T$ and $[S, \Delta_R]^T$, and these are diagonalized by $O_a^T m_{\rho\phi}^2 O_a \equiv \text{Diag}[m_{h_1}, m_{h_2}]$ and $O_\alpha^T m_{S\Delta}^2 O_\alpha \equiv \text{Diag}[m_{H_1}, m_{H_2}]$ respectively, where the mixing source of O_α arises from the nontrivial quartic coupling $\lambda_0 \Phi^T (i\sigma_2) \Delta^\dagger \Phi S$ and each mass eigenstate can be written in terms of couplings of Higgs potential². Here we define mixing

¹ Notice here that the neutral component of L' cannot be a DM candidate, because it is ruled out by the direct detection search via Z boson portal.

² See Appendix in details.

matrices as

$$O_{a(\alpha)} = \begin{bmatrix} c_{a(\alpha)} & s_{a(\alpha)} \\ -s_{a(\alpha)} & c_{a(\alpha)} \end{bmatrix}, \quad s_a = \frac{2\lambda_{\Phi\varphi}vv'}{m_{h_1}^2 - m_{h_2}^2}, \quad s_\alpha = \frac{2\sqrt{2}\lambda_0v^2}{m_{H_1}^2 - m_{H_2}^2}, \quad (\text{II.3})$$

where $c(s)_{a(\alpha)}$ is the short-hand notation of $\cos(\sin)_{a(\alpha)}$. Notice here that we assume small mixing case $O_a \approx \mathbf{1}$ in following analysis, which could however be a natural assumption because $s_a \lesssim 0.4$ is indicated from the data of LHC experiment [20–23]; therefore we take $m_\rho \approx m_{h_1}$ and $m_\phi \approx m_{h_2} \equiv m_{h_{SM}}$.

After the $\mu - \tau$ gauge symmetry breaking, *vector-like fermion mass matrix* can be written in the basis $[L'_e, L'_\mu, L'_\tau]^T$ as follows:

$$M_{L'} \equiv \begin{bmatrix} M_e & M_{e\mu} & M_{e\tau} \\ M_{e\mu} & M_\mu & 0 \\ M_{e\tau} & 0 & M_\tau \end{bmatrix}, \quad (\text{II.4})$$

where we have simply assumed $M_{L'}$ to be a real symmetric matrix and define $M_{e\mu} \equiv y_{E_1}v'/\sqrt{2}$ and $M_{e\tau} \equiv y_{E_2}v'/\sqrt{2}$. Then $M_{L'}$ is diagonalized by orthogonal mixing matrix V ($VV^T = 1$) as

$$V^T M_{L'} V = D_N \equiv \text{Diag.} [M_1, M_2, M_3], \quad N_{e,\mu,\tau} = V N_{1,2,3}, \quad (\text{II.5})$$

where $M_{1,2,3}$ is the mass eigenstate.

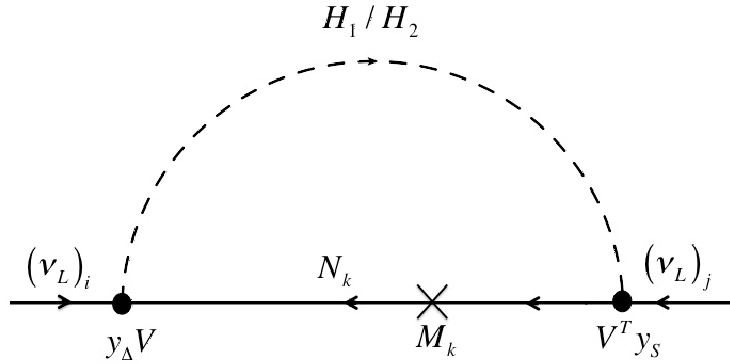


FIG. 1: The Feynman diagram for generating neutrino mass matrix.

A. Active neutrino mass and lepton flavor violating processes

Our active neutrino mass matrix is given in general at one-loop level by the diagram shown in Fig. 1 which is calculated as [19]

$$m_\nu^{th} = y_\Delta \epsilon V D_N R V^T y_S + [y_\Delta \epsilon V D_N R V^T y_S]^T, \quad (\text{II.6})$$

$$\epsilon \equiv \begin{bmatrix} 1 & 0 & 0 \\ 0 & 0 & 1 \\ 0 & 1 & 0 \end{bmatrix}, \quad R = \frac{s_\alpha c_\alpha}{(4\pi)^2} \left[\frac{r_{k_2} \ln r_{k_2}}{1 - r_{k_2}} - \frac{r_{k_1} \ln r_{k_1}}{1 - r_{k_1}} \right], \quad (\text{II.7})$$

where $r_{k_i} \equiv (m_{H_i}/M_k)^2$, ($i=1,2$), y_S and y_Δ are diagonal Yukawa matrices respectively. Here we derived neutrino mass formula using mass eigenstates of scalar bosons and exotic fermions; then the vertices in the diagram are products of coupling $y_{\Delta,S}$ and mixing matrix V , and contribution from λ_0 coupling with the SM Higgs VEV insertions is included in the scalar mixing s_α as Eq.(II.3). On the other hand, the neutrino mass matrix can be written in terms of experimental values as $m_\nu^{exp} = U D^\nu U^T$,³ where U is 3 by 3 unitary mixing matrix and $D^\nu \equiv \text{diag.}[m_{\nu_1} e^{i\rho}, m_{\nu_2} e^{i\sigma}, m_{\nu_3}]$ is neutrino mass eigenvalues [24]. Therefore we have to satisfy the relation $m_\nu^{th} \approx m_\nu^{exp}$. The smallness of neutrino masses $\sim 10^{-12}$ GeV partly arises from loop suppression factor and small mixing of $s_\alpha \sim 0.1$; $s_\alpha c_\alpha / (4\pi)^2 \sim 10^{-3}$, but the other factor is controlled by Yukawa couplings; $y_\Delta y_S \sim 10^{-11}$ for $D_N \approx \mathcal{O}(100)$ GeV. Thus each of Yukawa couplings could typically be the same order of electron Yukawa coupling; $y_\Delta \sim y_S \sim 10^{-5}$. On the other hand the mass hierarchy between M and m_{H_a} does not severely affect the order of neutrino masses.

Lepton flavor violations(LFVs) arises from the term y_Δ and y_S at one-loop level, and its

³ In the current experiment, only five parameters are measured; two mass difference squared and three mixing angles.

form can be given by

$$\text{BR}(\ell_i \rightarrow \ell_j \gamma) = \frac{48\pi^3 \alpha_{\text{em}} C_{ij}}{G_F^2 m_{\ell_i}^2} (|a_{R_{ij}}|^2 + |a_{L_{ij}}|^2), \quad (\text{II.8})$$

$$a_{R_{ij}} = \frac{1}{(4\pi)^2} \sum_{k=1,2,3} \left[\frac{Y_{\Delta_{ki}}^\dagger Y_{\Delta_{jk}}}{2} (m_{\ell_j} F_2[M_k, m_{\Delta^\pm}] + 2m_{\ell_i} (2F_2[M_k, m_{\Delta^{\pm\pm}}] + F_2[m_{\Delta^{\pm\pm}}, M_k])) \right. \\ \left. - Y_{S_{ki}}^\dagger Y_{S_{jk}} m_{\ell_i} (c_\alpha^2 F_2[H_1, M_k] + s_\alpha^2 F_2[H_2, M_k]) \right], \quad (\text{II.9})$$

$$a_{L_{ij}} = \frac{1}{(4\pi)^2} \sum_{k=1,2,3} \left[\frac{Y_{\Delta_{ki}}^\dagger Y_{\Delta_{jk}}}{2} (m_{\ell_i} F_2[M_k, m_{\Delta^\pm}] + 2m_{\ell_j} (2F_2[M_k, m_{\Delta^{\pm\pm}}] + F_2[m_{\Delta^{\pm\pm}}, M_k])) \right. \\ \left. - Y_{S_{ki}}^\dagger Y_{S_{jk}} m_{\ell_j} (c_\alpha^2 F_2[H_1, M_k] + s_\alpha^2 F_2[H_2, M_k]) \right], \quad (\text{II.10})$$

$$F_2(m_a, m_b) = \frac{2m_a^6 + 3m_a^4 m_b^2 - 6m_a^2 m_b^4 + 6m_b^6 + 12m_a^4 m_b^2 \ln(m_b/m_a)}{12(m_a^2 - m_b^2)^4}, \quad (\text{II.11})$$

where $Y_\Delta \equiv y_\Delta \epsilon V$, $Y_S \equiv y_S V$, η^\pm is the singly charged component of η , $G_F \approx 1.17 \times 10^{-5} [\text{GeV}]^{-2}$ is the Fermi constant, $\alpha_{\text{em}} \approx 1/137$ is the fine structure constant, $C_{21} \approx 1$, $C_{31} \approx 0.1784$, and $C_{32} \approx 0.1736$. Experimental upper bounds are respectively given by $\text{BR}(\mu \rightarrow e \gamma) \lesssim 4.2 \times 10^{-13}$, $\text{BR}(\tau \rightarrow e \gamma) \lesssim 3.3 \times 10^{-8}$, and $\text{BR}(\tau \rightarrow \mu \gamma) \lesssim 4.4 \times 10^{-8}$.

New contributions to the muon anomalous magnetic moment (muon $g-2$: Δa_μ) arises from Yukawa terms y_Δ with negative contribution and y_S with positive contribution. Also another source via additional gauge sector can also be induced by

$$\Delta a_\mu = \Delta a_\mu^{\text{Yukawa}} + \Delta a_\mu^{Z'}, \quad (\text{II.12})$$

$$\Delta a_\mu^{\text{Yukawa}} = -m_\mu [a_R + a_L]_{\mu\mu}, \quad \Delta a_\mu^{Z'} \approx \frac{g_{Z'}^2}{8\pi^2} \int_0^1 da \frac{2ra(1-a)^2}{r(1-a)^2 + a}, \quad (\text{II.13})$$

where $r \equiv (m_\mu/M_{Z'})^2$, and Z' is the new gauge vector boson. Thus we could explain the sizable muon $g-2$ ($\approx \mathcal{O}[10^{-9}]$) [3], if we can satisfy the constraint of trident process. Notice here that $g_{Z'} \lesssim 10^{-3}$ [27] has to be satisfied due to the trident process.

It is worthwhile to estimate three body decays; $\text{BR}(\tau \rightarrow \mu \bar{\mu} e)$ and $\text{BR}(\tau \rightarrow \mu \bar{\mu} \mu)$ via Z' boson at one-loop level in Fig. 2; tree level contribution from Z' is absent since Z' -charged lepton interactions are flavor diagonal. Then our formula is evaluated by [29]

$$\text{BR}(\tau \rightarrow \mu \bar{\mu} \ell) \approx \frac{N_\ell m_\tau^5}{768\pi^3 \Gamma_\tau} \left(\frac{g_{Z'}}{4\pi M_{Z'}} \right)^4 |G_2(y_S, V, M, m_S)|^2, \quad (\text{II.14})$$

where $G_2 \lesssim 0.1$ includes a loop function, $m_\tau \approx 1.777 \text{ GeV}$, $\Gamma_\tau \approx 2.3 \times 10^{-13} \text{ GeV}$, $N_\ell = 1$ for $\ell = e$ and $N_\ell = 1/2$ for $\ell = \mu$. Once we put typical values into the above formula, one

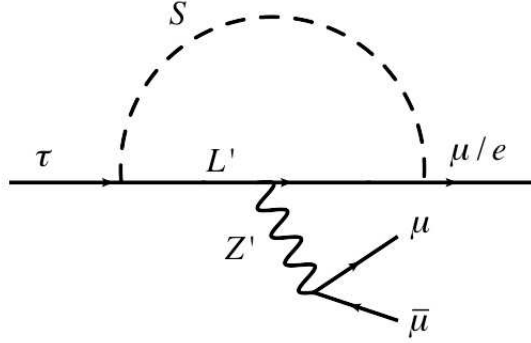


FIG. 2: The Feynman diagram for three body LFV decay via Z' .

finds to be

$$\text{BR}(\tau \rightarrow \mu \bar{\mu} \ell) \approx \mathcal{O}(10^{-10}), \quad (\text{II.15})$$

where we have adopted $g'/M_{Z'} \approx 1/(400 \text{ GeV})$ and $y_S V \approx \mathcal{O}(1)$. Since the experimental upper bounds are of the order 10^{-8} [30], our model does not restrict these modes for whole the parameters.

B. Dark matter

Here we consider the lightest inert boson $X \equiv H_1 \approx S$, assuming $s_\alpha \ll 1$ for simplicity. As we commented in previous subsection, this small mixing plays a role of suppression factor in neutrino mass formula while mass relation does not give significant change in the neutrino mass. Then annihilation modes generally arise from interactions associated with coupling constants y_Δ and y_S , and SM-Higgs portal. However we found that Yukawa modes cannot explain the sizable relic density; Its cross section is of the order $10^{-10} \text{ GeV}^{-2}$ at most, even when large coupling y_S is favor of the muon $g = 2$. Thus we should rely on interactions in the scalar sector to explain thermal relic density of DM. Then we focus on interactions between h_1 and X since the SM Higgs portal interaction is highly constrained by the direct detection experiments. Before considering the relic density, we also have to discuss the direct detection bound for h_1 portal coupling. The stringent bound comes from spin independent

nucleon-DM scattering via the h_1 scalar boson portal,⁴ and its cross section is evaluated as

$$\sigma_{SI} \approx (3.21 \times 10^{-29}) \times \frac{m_N^4 \lambda_{\varphi S}^2 s_a^2 c_a^2 \text{ GeV}^2}{4\pi m_{h_1}^4 (m_N + M_X)^2} \text{ cm}^2, \quad (\text{II.16})$$

where $\lambda_{\varphi S}$ is coefficient of $|\varphi|^2 S^2$, and $m_N \approx 0.939$ GeV is neutron mass. The recent experiment LUX [31] provides the bound on the scattering cross section as $\sigma_{SI} \lesssim 2.8 \times 10^{-46} \text{ cm}^2$ at $M_X \approx 110$ GeV. This can be interpreted by the following bound

$$\lambda_{\varphi S} s_a \lesssim 0.021, \quad (\text{II.17})$$

where we have used $m_{h_1} = 125$ GeV as a reference value and $c_a \sim 1$ is assumed. Hereafter we apply $\text{Max}[s_a \lambda_{\varphi S}] = 0.021$ in the analysis of relic density.

Relic density: The relevant annihilation cross sections to explain the relic density arise from the same coupling $\lambda_{\varphi S}$ in the scalar sector; $2X \rightarrow 2h_2, 2Z, W^+W^-, t\bar{t}$. Note here that the other modes such as $2X \rightarrow b\bar{b}$ are sufficiently small than the dominant modes, since its related coupling of b is of the order 10^{-2} at most. Then the dimensionless cross section $W(s)$ is given by

$$\begin{aligned} W(s) = & \frac{\lambda_{\varphi S}^2}{16\pi} \left(\frac{s_a^2}{|s - m_{h_1}^2 + im_{h_1}\Gamma_{h_1}|^2} \left[\sum_{V=Z,W} 4m_V^4 \sqrt{1 - \frac{4m_V^2}{s}} \left(3 - \frac{s}{m_V^2} + \frac{s^2}{4m_V^2} \right) \right. \right. \\ & \left. \left. + 6m_t^2 \sqrt{1 - \frac{4m_t^2}{s}} (s - 4m_t^2) \right] + \frac{1}{\pi} \sqrt{1 - \frac{4m_{h_2}^2}{s}} \int d\Omega \left| s_a^2 + \frac{\lambda_{\Phi\varphi} v_{\varphi} v}{4} \frac{1}{s - m_{h_1}^2 + im_{h_1}\Gamma_{h_1}} \right. \right. \\ & \left. \left. + 3 \frac{\lambda_{\Phi} s_a v^2}{2} \frac{1}{s - m_{h_2}^2 + im_{h_2}\Gamma_{h_2}} + \frac{\lambda_{\varphi S} s_a^2 v^2}{4} \left(\frac{1}{t - M_X^2} + \frac{1}{u - M_X^2} \right) \right|^2 \right), \quad (\text{II.18}) \end{aligned}$$

where s, t, u are Mandelstam variables, $c_a \simeq 1$ is taken, we have assumed narrow width of $h_{1/2}$ as $\Gamma_{h_{1/2}} \ll m_{h_{1/2}}$ GeV, and fixed $m_t \approx 172.44$ GeV, $m_Z \approx 91.2$ GeV, $m_W \approx 80.4$ GeV. Then the relic density of DM is given by [33]

$$\Omega h^2 \approx \frac{1.07 \times 10^9}{\sqrt{g_*(x_f)} M_{Pl} J(x_f) [\text{GeV}]}, \quad (\text{II.19})$$

where $g^*(x_f \approx 25) \approx 100$ is the degrees of freedom for relativistic particles at the freeze-out temperature $T_f = M_X/x_f$, $M_{Pl} \approx 1.22 \times 10^{19}$ GeV, and $J(x_f) (\equiv \int_{x_f}^{\infty} dx \frac{\langle \sigma v_{\text{rel}} \rangle}{x^2})$ is given

⁴ Note here that the SM Higgs h_2 portal does not satisfy the relic density and direct detection simultaneously [28] except the pole DM mass at $m_{h_2}/2$ and we assume $\lambda_{\Phi S}$ to be small to avoid constraints from direct detection.

by [36]

$$J(x_f) = \int_{x_f}^{\infty} dx \left[\frac{\int_{4M_X^2}^{\infty} ds \sqrt{s - 4M_X^2} W(s) K_1\left(\frac{\sqrt{s}}{M_X} x\right)}{16M_X^5 x [K_2(x)]^2} \right]. \quad (\text{II.20})$$

Then one has to satisfy the current relic density of DM; $\Omega h^2 \approx 0.12$ [34]. In our numerical analysis below we focus on annihilation mode of $2X \rightarrow \{ZZ, W^+W^-, t\bar{t}, 2h_2\}$ assuming m_{h_1} to be heavy. Also we have assumed other scalar contact interactions such as $\lambda_{\Phi S}$ is small, and we have neglected mixing between $Z - Z'$, thus we do not consider the modes $2X \rightarrow Z'Z'$.

III. NUMERICAL ANALYSIS

In this section, we show a global analysis, where we have fixed some parameters for simplicity. At first, we fix $m_{H_2} = m_{\Delta^\pm} = m_{\Delta^{\pm\pm}}$ in order to evade the constraints from oblique parameters in the triplet boson; the S, T, U-parameters are suppressed when the masses in the triplet are degenerated [35]. Also we numerically solve our parameters $Y \equiv (y_{S_e}, y_{S_\mu}, y_{S_\tau}, y_{\Delta_2}, y_{\Delta_3})$, by using the relation $m_\nu^{th} = m_\nu^{exp}$,⁵ where we impose the perturbative bounds on these output parameters; $Y \lesssim \sqrt{4\pi}$. Thus we randomly select the following range of reduced input parameters as

$$100 \text{ GeV} \leq M_X \text{ GeV}, \quad m_{H_2} \in [1.2M_X, 2500] \text{ GeV},$$

$$|y_{\Delta_1}| \in [0.1, 4\pi], \quad (\rho, \sigma) \in [0, \pi], \quad \delta \in [\pi, 2\pi], \quad |s_\alpha| \in [10^{-5}, 0.1], \quad (\text{III.1})$$

$$M_{Z'} \in [10^{-3}, 10^3] \text{ [GeV]}, \quad g_{Z'} \in [10^{-5}, 10^{-3}], \quad (\text{III.2})$$

where we have used experimental neutrino oscillation data in ref. [25] with 3σ range. In Fig. 3, we show the scattering allowed plots in terms of muon $g - 2$ and M_X to satisfy the neutrino oscillation data and LFVs, where green region is in good agreement with the current experimental data $(26.1 \pm 8.0) \times 10^{-10}$. It shows that there is allowed region simultaneously to satisfy the muon $g - 2$ and relic density of DM.

In Fig. 4, we show the allowed scattering plots in terms of sum of neutrino masses and m_{ν_1} . It suggests that the lightest neutrino mass is of the order 10^{-12} eV.

⁵ In principle, six parameters can numerically be solved, but it is technically difficult in our model.

In Fig. 5, we demonstrate Majorana phases; ρ (with red points) and σ (with blue points) in terms of Dirac phase δ , where the red/blue present the region in $M_X \in [100, 350]$ GeV.⁶ It displays that δ runs over $\pi \sim 2\pi$, whereas Majorana phases tend to be localized, depending on ρ and σ . Especially, both of these phases are in favor of being localized at around $\pi/2$ that could be one of the remarkable features of this model.

In fig. 6, we show the line of relic density in term of the DM mass, where we have used $\text{Max}[\lambda_{\varphi S S_a}] = 0.02$, and horizontal line represents the measured relic density ~ 0.12 . Here the blue, red, and green line respectively represent the h_1 mass of 200 GeV, 400 GeV, and 600 GeV. Since the mass of h_1 is not constrained by any experiments discussed above, there are solutions in the whole mass range of DM that we have taken.

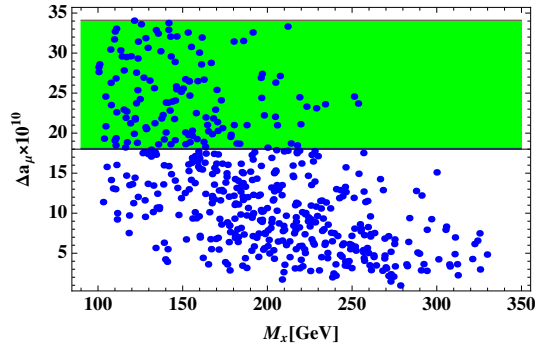


FIG. 3: Scattering plots in terms of muon $g - 2$ and M_X to satisfy the neutrino oscillation data and LFVs, where green region is in good agreement with the current experimental data $(26.1 \pm 8.0) \times 10^{-10}$.

⁶ Here we take the upper bound 350 GeV on M_X . This is simply because the larger mass region than 250 GeV does not satisfy the sizable muon $g - 2$ from loop diagram containing DM.

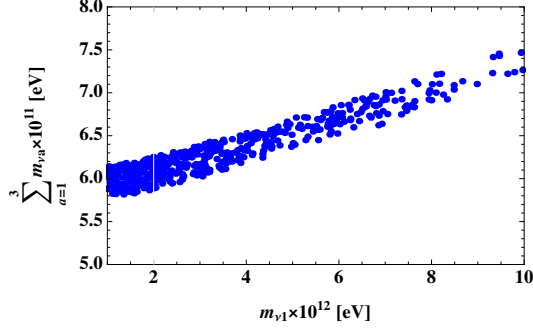


FIG. 4: Scattering plots in terms of sum of neutrino masses and $m_{\nu 1}$ in the left panel and Dirac phase δ and Majorana phases; ρ (with red points) and σ (with blue points), in the right panel.

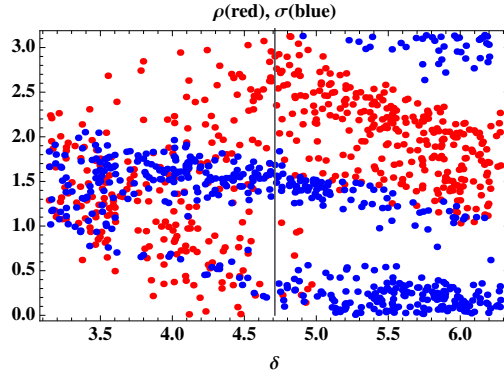


FIG. 5: Scattering plots in terms of sum of neutrino masses and $m_{\nu 1}$ in the left panel and Dirac phase δ and Majorana phases; ρ (with red points) and σ (with blue points), in the right panel.

Comment on the specific case: It is worth mentioning the following two hypotheses that lead a predictive two-zero texture with $(m_\nu)_{22} = (m_\nu)_{33} = 0$:

$$i) \quad M \equiv M_1 \approx M_2 \approx M_3, \quad (\text{III.3})$$

$$ii) \quad y_{S_2} \approx y_{\Delta_3} \approx 0, \text{ or } y_{S_3} \approx y_{\Delta_2} \approx 0. \quad (\text{III.4})$$

The case *i*) suggests that a fermion DM is in a coannihilation system to satisfy the correct relic density of Universe when $M < m_{H_{1,2}}$. Notice here that the lower mass bound on M is around 100 GeV from the LEP experiment. Transversely a bosonic DM candidate can simply satisfy the relic density.

The case *ii*) suggests that a fermion DM does not require a coannihilation process among

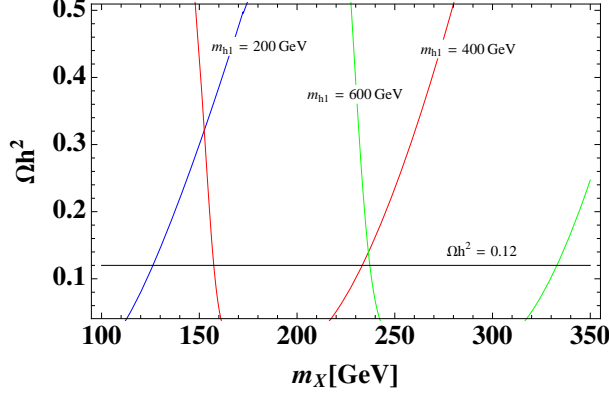


FIG. 6: Plot line of relic density in term of the DM mass, where we have used $\text{Max}[\lambda_{\varphi S s_a}] = 0.02$, and horizontal line represents the measured relic density ~ 0.12 . Here the blue, red, and green line respectively represent the h_1 mass of 200 GeV, 400 GeV, and 600 GeV.

neutral fermions, however it must still be considered between the exotic charged fermions E due to the constraint of oblique parameter.

In both of the cases, the situation could be more or less same if we identify DM as the bosonic DM candidate, and we adopt *i*) in our discussion below. Before starting the discussion of neutrinos, let us roughly estimate the degree of our predictability from $\mu - \tau$ symmetry. Since we have eleven free parameters (three in y_S , three in y_Δ , and five in $M_{L'}$) which contribute to form the texture, it still seems to remain nine free parameters even after imposing the above conditions *i*) or *ii*). Thus naive expectation gives no predictions while one finds the type-C of neutrino texture that has only seven parameters. It suggests that two more freedom in the parameter sets are reduced by our specific textures of y_S , y_Δ , and $M_{L'}$ which are determined by the $\mu - \tau$ symmetry. Thus our model still improve predictability

by two degrees of freedom due to the symmetry.⁷ Then m_ν is simplified as

$$\begin{aligned}
m_\nu &\approx R [y_\Delta \epsilon (V D_N V^T) y_S + y_S (V D_N V^T) \epsilon y_\Delta] \\
&= R (y_\Delta \epsilon M_{L'} y_S + y_S M_{L'} \epsilon y_\Delta) \\
&= R \begin{bmatrix} 2M_e y_{S_e} y_{\Delta_1} & M_{e\tau} y_{S_e} y_{\Delta_2} + M_{e\mu} y_{S_\mu} y_{\Delta_1} & M_{e\mu} y_{S_e} y_{\Delta_3} + M_{e\tau} y_{S_\tau} y_{\Delta_1} \\ M_{e\tau} y_{S_e} y_{\Delta_2} + M_{e\mu} y_{S_\mu} y_{\Delta_1} & 0 & M_\mu y_{S_\mu} y_{\Delta_3} + M_\tau y_{S_\tau} y_{\Delta_2} \\ M_{e\mu} y_{S_e} y_{\Delta_3} + M_{e\tau} y_{S_\tau} y_{\Delta_1} & M_\mu y_{S_\mu} y_{\Delta_3} + M_\tau y_{S_\tau} y_{\Delta_2} & 0 \end{bmatrix}
\end{aligned} \tag{III.5}$$

$$\approx \begin{bmatrix} 0.022 - 0.75 & 0.028 - 0.039 & 0.030 - 0.040 \\ 0.028 - 0.039 & 0 & 0.023 - 0.75 \\ 0.030 - 0.040 & 0.023 - 0.75 & 0 \end{bmatrix} [\text{eV}], \tag{III.6}$$

where we have used $V D_N V^T = V V^T M_{L'} V V^T = M_{L'}$. Eq. (III.5) corresponds to the type C two zero texture that provides several predictions that only an inverted neutrino mass ordering is allowed and specific pattern of phases. In fig. 7, we show ρ (red) and σ (blue) in terms of δ , where we adapt the recent global neutrino oscillation data [25] up to 3σ confidence level and the same input value in the general analysis. It implies that the region of ρ is restricted to be $0 \sim 3\pi/2$, whereas σ be $3\pi/2 \sim 2\pi$, and these are overlapped at around $\delta = 3\pi/2$ that is in good agreement with the current neutrino experiments as the best fit value. In this case, the dominant contribution of muon $g-2$ arises from $\Delta a_\mu^{Z'}$, where $g_{Z'} \lesssim 10^{-3}$ [27] is satisfied due to the trident process. While the relic density of DM can be obtained by the Yukawa coupling y_S that leads to the d-wave dominant. This result is opposite to the one of general feature, although we do not show the detailed analysis here because this is nothing but ad-hoc hypothesis.

IV. CONCLUSIONS AND DISCUSSIONS

We have proposed a radiative seesaw model at one-loop level with a flavor dependent gauge symmetry $U(1)_{\mu-\tau}$, in which we have consider gauge singlet-like bosonic dark matter

⁷ Even if the general matrix case of $M_{L'}$ has eleven parameters (seven reals and four imaginaries), the two predictabilities does not changes, therefore one finds type-C of the neutrino texture due to reductions of eight parameters.

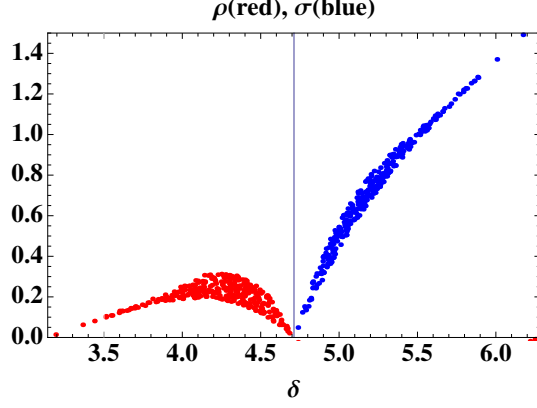


FIG. 7: The allowed region between ρ (red) and σ (blue) in terms of δ , where we adapt the recent global neutrino oscillation data [25] up to 3σ confidential level and the same input value in the general analysis. It implies that the region of ρ is restricted to be $0 \sim 3\pi/2$, whereas σ $3\pi/2 \sim 2\pi$, and these are overlapped at around $\delta = 3\pi/2$ that is the best fit value in the current neutrino experiments.

candidate and explained muon $g - 2$ without conflict of LFVs. In the numerical analysis, we have shown several features as follows:

1. Whole the DM mass region with $\lambda_{\varphi S S_a} \approx 0.021$ is obtained by the experimental bounds on spin independent scattering and relic density of DM. And this range is in good agreement with the current experimental data of muon $g - 2$ without conflict of LFVs as well as neutrino oscillation data.
2. The typical lightest neutrino mass is of the order 10^{-12} eV.
3. There exist a mild correlation between the Dirac phase δ and Majorana phases ρ, σ . Therefore, δ runs over $\pi \sim 2\pi$, whereas Majorana phases tend to be localized, depending on ρ and σ . Especially, both of these phases are in favor of being localized at around $\pi/2$.
4. As a specific case such as $M \equiv M_1 \approx M_2 \approx M_3$, we have found the predictive two zero texture(type-C) and their features are clearer than the generic one. As an example, the region of ρ is restricted to be $0 \sim 3\pi/2$, whereas σ be $3\pi/2 \sim 2\pi$, and these are overlapped at around $\delta = 3\pi/2$ that is in good agreement with the current neutrino experiments as the best fit value.

Finally, we have an inert doubly charged Higgs boson which decay into dark matter and SM fermions by cascade decay modes. It will be interesting to search for the signal of "missing E_T + same sign leptons" as a signature of the inert Higgs triplet as well as our dark matter. The detailed analysis of the signal is beyond the scope of this paper and it will be studied elsewhere.

If global $U(1)_{\mu-\tau}$ symmetry is applied to our model, a few results could change. The first one is that the muon $g - 2$ due to the absence of Z' contribution. The second one is that a new annihilation mode of DM relic density has to be added; $2X \rightarrow 2G$, where G is a physical massless goldstone boson. As a result, the allowed range of DM mass is wider, since whole the cross section increases.

Appendix

Here we give the most general Higgs potential in a renormalizable theory as

$$\begin{aligned}
\mathcal{V} = & m_\Phi^2 \Phi^\dagger \Phi + m_\varphi^2 \varphi^* \varphi + m_\Delta^2 \text{Tr}[\Delta^\dagger \Delta] + \frac{1}{2} m_S^2 S^2 \\
& + (\lambda_0 \Phi^T (i\sigma_2) \Delta^\dagger \Phi S + \text{c.c.}) + \lambda_\Phi |\Phi^\dagger \Phi|^2 + \lambda_\varphi |\varphi^* \varphi|^2 + \lambda_\Delta (\text{Tr}[\Delta^\dagger \Delta])^2 + \lambda'_\Delta \text{Det}[\Delta^\dagger \Delta] + \frac{1}{4!} \lambda_S S^4 \\
& + \lambda_{\Phi\varphi} (\Phi^\dagger \Phi) (\varphi^* \varphi) + \lambda_{\Phi\Delta} (\Phi^\dagger \Phi) \text{Tr}[\Delta^\dagger \Delta] + \lambda'_{\Phi\Delta} \sum_{i=1-3} (\Phi^\dagger \tau_i \Phi) \text{Tr}[\Delta^\dagger \tau_i \Delta] + \frac{1}{2} \lambda_{\Phi S} (\Phi^\dagger \Phi) S^2 \\
& + \lambda_{\varphi\Delta} \varphi^* \varphi \text{Tr}[\Delta^\dagger \Delta] + \frac{1}{2} \lambda_{\varphi S} \varphi^* \varphi S^2 + \frac{1}{2} \lambda_{\Delta S} \text{Tr}[\Delta^\dagger \Delta] S^2.
\end{aligned} \tag{IV.1}$$

Acknowledgments

H. O. is sincerely grateful for all the KIAS members.

-
- [1] A. Crivellin, G. D'Ambrosio and J. Heeck, Phys. Rev. D **91**, no. 7, 075006 (2015) [arXiv:1503.03477 [hep-ph]].
 - [2] C. Kownacki, E. Ma, N. Pollard and M. Zakeri, arXiv:1611.05017 [hep-ph].
 - [3] G. W. Bennett *et al.* [Muon G-2 Collaboration], Phys. Rev. D **73**, 072003 (2006) [hep-ex/0602035].

- [4] X. G. He, G. C. Joshi, H. Lew and R. R. Volkas, Phys. Rev. D **43**, 22 (1991); D **44**, 2118 (1991).
- [5] S. Baek, N. G. Deshpande, X. G. He and P. Ko, Phys. Rev. D **64**, 055006 (2001) [hep-ph/0104141].
- [6] E. Ma, D. P. Roy and S. Roy, Phys. Lett. B **525**, 101 (2002) [hep-ph/0110146].
- [7] E. J. Chun and K. Turzyski, Phys. Rev. D **76**, 053008 (2007) [hep-ph/0703070].
- [8] S. Baek and P. Ko, JCAP **0910**, 011 (2009) [arXiv:0811.1646 [hep-ph]].
- [9] K. Harigaya, T. Igari, M. M. Nojiri, M. Takeuchi and K. Tobe, JHEP **1403**, 105 (2014) [arXiv:1311.0870 [hep-ph]].
- [10] W. Altmannshofer, S. Gori, M. Pospelov and I. Yavin, Phys. Rev. D **89**, 095033 (2014) [arXiv:1403.1269 [hep-ph]].
- [11] J. Heeck, M. Holthausen, W. Rodejohann and Y. Shimizu, Nucl. Phys. B **896**, 281 (2015) [arXiv:1412.3671 [hep-ph]].
- [12] T. Araki, F. Kaneko, Y. Konishi, T. Ota, J. Sato and T. Shimomura, Phys. Rev. D **91**, no. 3, 037301 (2015) [arXiv:1409.4180 [hep-ph]].
- [13] S. Baek, H. Okada and K. Yagyu, JHEP **1504**, 049 (2015) [arXiv:1501.01530 [hep-ph]].
- [14] T. Araki, F. Kaneko, T. Ota, J. Sato and T. Shimomura, Phys. Rev. D **93**, no. 1, 013014 (2016) [arXiv:1508.07471 [hep-ph]].
- [15] S. Baek, Phys. Lett. B **756**, 1 (2016) [arXiv:1510.02168 [hep-ph]].
- [16] P. Ko, T. Nomura and H. Okada, arXiv:1701.05788 [hep-ph].
- [17] P. Ko, T. Nomura and H. Okada, arXiv:1702.02699 [hep-ph].
- [18] W. Altmannshofer, C. Y. Chen, P. S. Bhupal Dev and A. Soni, Phys. Lett. B **762**, 389 (2016) [arXiv:1607.06832 [hep-ph]].
- [19] H. Okada and Y. Orikasa, Phys. Rev. D **94**, no. 5, 055002 (2016) [arXiv:1512.06687 [hep-ph]].
- [20] The numerical analyses on the Higgs decays are performed using the program **HDECAY**: A. Djouadi, J. Kalinowski and M. Spira, Comput. Phys. Commun. 108 (1998) 56; A. Djouadi, M. Muhlleitner and M. Spira, Acta. Phys. Polon. B38 (2007) 635.
- [21] S. Choi, S. Jung and P. Ko, JHEP **1310**, 225 (2013) [arXiv:1307.3948 [hep-ph]].
- [22] K. Cheung, P. Ko, J. S. Lee and P. Y. Tseng, JHEP **1510**, 057 (2015) [arXiv:1507.06158 [hep-ph]].
- [23] G. Dupuis, JHEP **1607**, 008 (2016) [arXiv:1604.04552 [hep-ph]].

- [24] H. Fritzsch, Z. z. Xing and S. Zhou, JHEP **1109**, 083 (2011) [arXiv:1108.4534 [hep-ph]].
- [25] D. V. Forero, M. Tortola and J. W. F. Valle, Phys. Rev. D **90**, no. 9, 093006 (2014) [arXiv:1405.7540 [hep-ph]].
- [26] Talk by Konosuke Iwamoto (T2K Collaboration) at the ICHEP 2016, Chicago, August 2016.
- [27] W. Altmannshofer, S. Gori, M. Pospelov and I. Yavin, Phys. Rev. Lett. **113**, 091801 (2014) [arXiv:1406.2332 [hep-ph]].
- [28] S. Kanemura, S. Matsumoto, T. Nabeshima and N. Okada, Phys. Rev. D **82**, 055026 (2010) [arXiv:1005.5651 [hep-ph]].
- [29] A. Crivellin, S. Najjari and J. Rosiek, JHEP **1404**, 167 (2014) [arXiv:1312.0634 [hep-ph]].
- [30] C. Patrignani *et al.* [Particle Data Group], Chin. Phys. C **40**, no. 10, 100001 (2016).
- [31] D. S. Akerib *et al.* [LUX Collaboration], Phys. Rev. Lett. **118**, no. 2, 021303 (2017) [arXiv:1608.07648 [astro-ph.CO]].
- [32] M. Srednicki, R. Watkins and K. A. Olive, Nucl. Phys. B **310**, 693 (1988).
- [33] J. Edsjo and P. Gondolo, Phys. Rev. D **56**, 1879 (1997) [hep-ph/9704361].
- [34] P. A. R. Ade *et al.* [Planck Collaboration], Astron. Astrophys. **571**, A16 (2014) [arXiv:1303.5076 [astro-ph.CO]].
- [35] T. Nomura, H. Okada and Y. Orikasa, Phys. Rev. D **94**, no. 11, 115018 (2016) [arXiv:1610.04729 [hep-ph]].
- [36] K. Nishiwaki, H. Okada and Y. Orikasa, Phys. Rev. D **92**, no. 9, 093013 (2015) [arXiv:1507.02412 [hep-ph]].